INSTITUTE OF PHYSICS PUBLISHING JOURNAL OF OPTICS B: QUANTUM AND SEMICLASSICAL OPTICS
J. Opt. B: Quantum Semiclass. Opt. **4** (2002) S253–S259 PII: S1464-4266(02)37867-4

Puzzling aspects of Young interference and spontaneous intrinsic decoherence

Rodolfo Bonifacio and Stefano Olivares

Dipartimento di Fisica, Università degli Studi di Milano, INFM and INFN Sezione di Milano, via Celoria 16, I-20133 Milano, Italy

Received 1 January 2002
Published 29 July 2002
Online at stacks.iop.org/JOptB/4/S253

Abstract
We discuss the single-particle Young interference experiment in *position space*, showing its close relation with the time-dependent Schrödinger spread. In the two-slit case there is always a maximum at the centre of the screen. Here we demonstrate that, with three slits, one can have zero intensity (at the centre) for *discrete* values of the spacing between the slits and of the distance of the screen. Finally, we show the possibility that spontaneous intrinsic decoherence destroys the interference pattern and that decoherence becomes stronger at the macroscopic limit.

Keywords: Quantum mechanics, interference, atomic and molecular physics

(Some figures in this article are in colour only in the electronic version)

1. Introduction

Feynman [1] said that interference is *the only mystery* of the quantum mechanical world. In a previous work [2] we analysed quantum interference focusing our attention on a single-particle Young experiment: there we described interference pattern in position space, while in standard textbooks it is usually described solving the Schrödinger equation in momentum space, so that a *time-independent* angular distribution is obtained. We were able, in contrast, to explicitly see the time dependence of the interference pattern. In particular, Young interference is closely related to the free-particle *time-dependent* Schrödinger spread, a feature that does not appear in the momentum representation. Moreover, one can give an optical analogy by putting the evolution time $t = L/v$ at the end of the calculation, where L is the distance from the screen and v is the mean particle velocity [2]. In such a case, the usual Young interference pattern appears only for a time long enough to have complete overlap of the two wavepackets coming from the slits. What happens if one adds a third slit between the first two? The central peak vanishes and becomes a zero-intensity point for *discrete values of the spacings between the slits and of the distance of the screen*!

Moreover, since the interference pattern is time dependent, fluctuations of the evolution time $t = L/v$ induced by velocity spread give rise to decoherence [3, 4], i.e. to the reduction of fringe visibility. This is *spontaneous decoherence* because it is not induced by the interaction with the environment [5]. In [4] we have described spontaneous decoherence in cavity QED. Here velocity fluctuations can have experimental reasons due to thermal fluctuations or intrinsic ones due to the Heisenberg uncertainty principle (HUP). In the last case one has *spontaneous intrinsic decoherence* (SID). Furthermore, in [3], using the Tam Mandelstam inequality [6], it has been suggested that in SID these time fluctuations have an intrinsic inferior limit given by the *energy–time*

$$\tau_E \equiv \frac{\hbar}{2\Delta\mathcal{H}} \tag{1}$$

where $\Delta\mathcal{H}$ is the variance of the system Hamiltonian $\mathcal{H}$. In this paper we describe spontaneous decoherence in two- and three-slit Young interference experiments. The conditions to observe spontaneous decoherence due to classical (thermal) fluctuations of the particles velocity and SID, coming from the velocity spread due to HUP, are specified.

2. Three-slit Young interference

We consider a particle beam moving along the $\hat{z}$ axis with velocity $\overline{V}$ (see figure 1). Using the one-dimensional time-dependent Schrödinger equation and assuming that at time $t = 0$, when particles pass through the slits, the state is a superposition of three Gaussian wavepackets, at time t one has

$$\Psi(x,t) \propto \Psi_0(x,t) + \Psi_1(x,t) + \Psi_2(x,t) \tag{2}$$

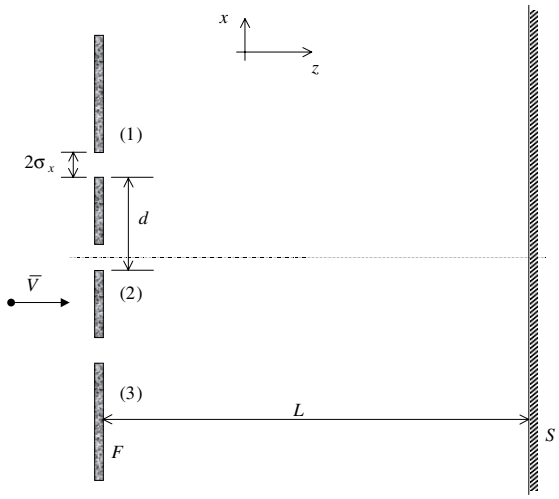

Figure 1. Setup of the three-slit Young experiment described in the text.

where $\Psi_j(x,t)$, $j = 0, 1, 2$, is given by [7]

$$\Psi_j(x,t) \propto \exp\left\{-\frac{(x-x_j)^2}{4\sigma(t)^2}\left(1-\mathrm{i}\frac{\sigma_v}{\sigma_x}t\right)\right\}, \qquad j=0,1,2 \tag{3}$$

with $x_1 = -x_2 = d$, $x_0 = 0$ and $\sigma(t) = \sqrt{\sigma_x^2 + \sigma_v^2 t^2}$, where $\sigma_x\sigma_v = \hbar/2m$. From now on, it is useful to introduce the dimensionless quantities

$$\overline{x} = \frac{x}{\sigma_x}, \qquad \overline{d} = \frac{d}{\sigma_x}, \qquad \overline{t} = \frac{\sigma_v t}{\sigma_x} = \frac{\hbar}{2m\sigma_x^2}t. \tag{4}$$

If we close the holes 1 and 3, the system is simply described by $\Psi_0(\overline{x},\overline{t})$, which *spreads* because of the free evolution ruled by the Schrödinger equation. This effect is known as *free-particle Schrödinger spread*. On the other hand, one can consider closing only the central slit, thus obtaining the usual two-slit Young interference experiment, as we shall show. In this case the initial wavefunction becomes

$$\Psi(x,t) \propto \Psi_1(x,t) + \Psi_2(x,t). \tag{5}$$

and the probability density $P(\overline{x},\overline{t})$ of finding a particle in $\overline{x}$ at time $\overline{t}$ is

$$P(\overline{x},\overline{t}) \equiv |\Psi(\overline{x},\overline{t})|^2 = |c(\overline{t})|^2\left(G_+ + G_- + 2\sqrt{G_+G_-}\cos\omega\overline{t}\right) \tag{6}$$

where $|c(\overline{t})|^2$ is a normalization factor and

$$G_\pm = \exp\left\{-\frac{(\overline{x}\pm\overline{d})^2}{2(1+\overline{t}^2)}\right\}, \qquad \omega = \frac{\overline{x}\overline{d}}{1+\overline{t}^2}. \tag{7}$$

The *time-dependent* interference term, $\cos\omega\overline{t}$, is modulated by

$$\sqrt{G_+G_-} = \exp\left\{-\frac{\overline{x}^2}{2(1+\overline{t}^2)}\right\}\exp\left\{-\frac{\overline{d}^2}{2(1+\overline{t}^2)}\right\} \tag{8}$$

and, under the condition

$$\overline{t} \gg \overline{d} \gg 1, \tag{9}$$

equation (8) can be approximated by

$$\sqrt{G_+G_-} \approx \exp\left\{-\frac{\overline{x}^2}{2\overline{t}^2}\right\}, \tag{10}$$

i.e. one has a Gaussian modulation and so the interference term is relevant only for $\overline{x} \ll \overline{t}$ ($x \ll \sigma_v t$). Furthermore, to see the leading role of Schrödinger spread, one must rewrite equation (9) using the scaling (4):

$$\sigma_v t \gg d \gg \sigma_x \tag{11}$$

which is the condition to have the complete overlap of the wavepackets: the interference pattern provides a direct evidence of the Schrödinger spread. Notice that the time dependence we obtained is a consequence of the time-dependent solution of the Schrödinger equation in *position space*: in standard textbooks, in contrast, such a solution is given in *momentum space*, obtaining only a *time-independent* angular distribution. The maxima occur at $\omega\overline{t} = 2n\pi$ (see equation (6)) so that by equations (7) and (4) we can write (in the limit of equation (9))

$$\overline{x}_n = \frac{2n\pi\overline{t}}{\overline{d}}. \tag{12}$$

Moreover, since the maxima are modulated by (see equation (10))

$$\exp\left\{-\frac{\overline{x}_n^2}{2\overline{t}^2}\right\} = \exp\left\{-\frac{1}{2}\left(\frac{2n\pi}{\overline{d}}\right)^2\right\} \tag{13}$$

the number of visible fringes is proportional to $\overline{d} = d/\sigma_x$ as in the optical case. In figure 2 we show the time evolution of the two-slit interference pattern.

Finally, when all the slits are opened, the wavefunction is given by equation (2) and the probability density of finding a particle on the screen S at position $\overline{x}$ is

$$\begin{aligned} P(\overline{x},\overline{t}) &\equiv |\Psi(\overline{x},\overline{t})|^2 \\ &= |\hat{c}(\overline{t})|^2\big(G_+ + G_- + G_0 + 2\sqrt{G_+G_-}\cos\omega_1\overline{t} \\ &\quad + 2\sqrt{G_0G_-}\cos\omega_2\overline{t} + 2\sqrt{G_+G_0}\cos\omega_3\overline{t}\big) \end{aligned} \tag{14}$$

where $|\hat{c}(\overline{t})|^2$ is a suitable normalization factor and

$$G_\pm = \exp\left\{-\frac{(\overline{x}\pm\overline{d})^2}{2(1+\overline{t}^2)}\right\}, \qquad G_0 = \exp\left\{-\frac{\overline{x}^2}{2(1+\overline{t}^2)}\right\}, \tag{15}$$

$$\omega_1 = \frac{\overline{x}\overline{d}}{1+\overline{t}^2}, \qquad \omega_2 = \frac{(\overline{x}-\overline{d}/2)(\overline{d}/2)}{1+\overline{t}^2}, \qquad \omega_2 = \frac{(\overline{x}+\overline{d}/2)(\overline{d}/2)}{1+\overline{t}^2}. \tag{16}$$

Specializing equation (14) for $\overline{x} = 0$, one has

$$|\Psi(0,\overline{t})|^2 = |\hat{c}(\overline{t})|^2\left\{1+4G+4\sqrt{G}\cos\left(\frac{\overline{d}^2}{4(1+\overline{t}^2)}\overline{t}\right)\right\} \tag{17}$$

with

$$G = \exp\left\{-\frac{\overline{d}^2}{2(1+\overline{t}^2)}\right\}. \tag{18}$$

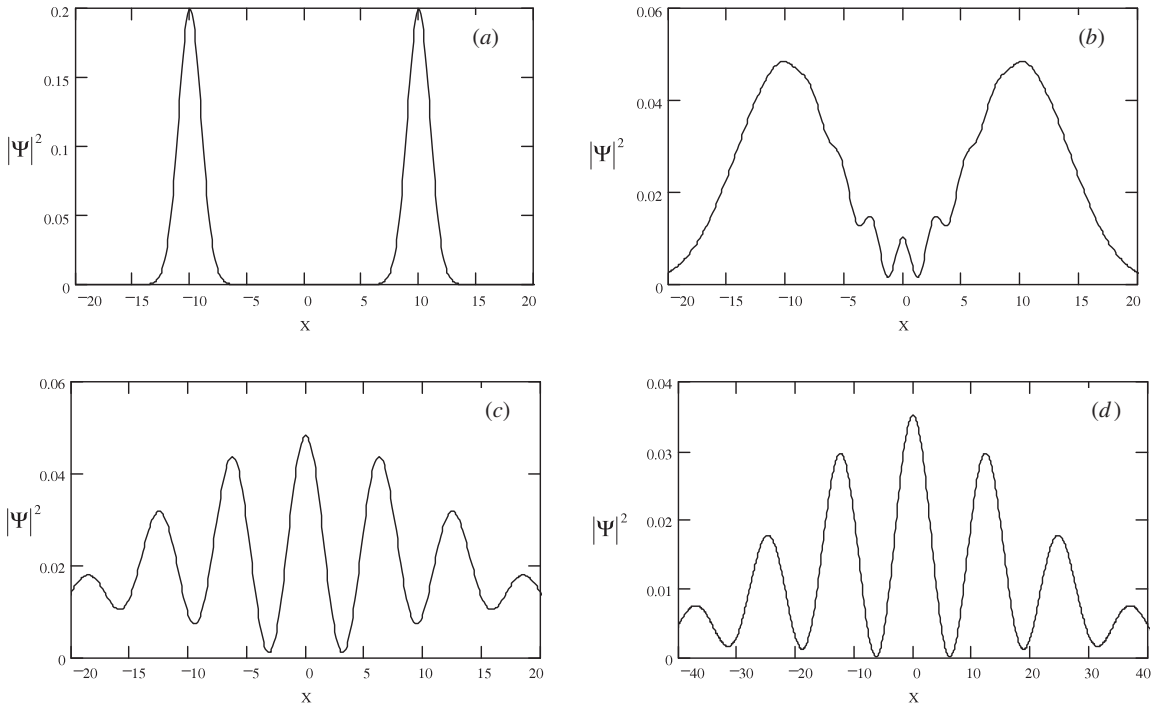

Figure 2. Time evolution of the two-slit interference pattern with $d/\sigma_x = 10$ for different values of the dimensionless time $\overline{t}$: (*a*) 0; (*b*) 4; (*c*) 10; (*d*) 20. Here $\overline{t} = \sigma_v t/\sigma_x = L/R$, where $R = 2\sigma_x^2/\hbar$ is the Rayleigh range.

Maxima and minima in $\overline{x} = 0$ are obtained imposing

$$\frac{\overline{d}^2}{4(1+\overline{t}^2)}\overline{t} = n\pi, \tag{19}$$

so one has maxima or minima for even or odd n, respectively. Moreover, the minimum of intensity is exactly equal to zero if we require $\sqrt{G} = 1/2$ (the physical meaning of this choice will be clarified in the next section), i.e.

$$\frac{\overline{d}^2}{2(1+\overline{t}^2)} = 2\ln(2). \tag{20}$$

Equations (19) and (20) bring us to the final conditions:

$$\overline{t}_n = \frac{\pi}{\ln(2)}n \approx 4.5n, \tag{21}$$

$$\overline{d}_n = 2\sqrt{\frac{(\ln(2))^2 + \pi^2 n^2}{\ln(2)}} \approx 7.7n. \tag{22}$$

In figure 3 we plot the comparison between the two- and three-slit cases for $n = 1$–3. This figure, for $n = 1$ and 3, explicitly shows that a new slit between the two slits of a Young experiment can inhibit particles from reaching a place where they had high probability to go, so no particle arrives at that point! The corresponding physical optical values of L and d directly come from relations $\overline{t} = L/R$ and $d = d/\sigma_x$, i.e.

$$L_n \approx 4.5Rn \tag{23}$$

$$d_n \approx 7.7\sigma_x n \tag{24}$$

where we recall that $\hbar = \hbar/m\overline{V}$ and $R = 2\sigma_x^2/\hbar$.

3. Optical analogy

Let us now consider the distribution $P(x, t)$ (coming from (6) using (4)) as the probability density of finding a particle on a screen S at distance L, such that $t = L/\overline{V}$, where $\overline{V}$ is the mean velocity perpendicular to the plane $\hat{x}$ of the slits (see figure 1). Equation (12) gives

$$\frac{x_n}{L} = \frac{\lambda}{2d}n \qquad \left(\lambda = \frac{h}{m\overline{V}} = 2\pi\hbar\right) \tag{25}$$

which is the usual optical condition for constructive interference assuming $\lambda \ll d \ll L$. All the equations of the previous section can be translated in optical terms identifying $t = L/\overline{V}$ and $\hbar = \hbar/m\overline{V}$. In particular, the conditions $\overline{d} \ll \overline{t}$ and $\overline{x} \ll \overline{t}$ become

$$\frac{d}{L} \ll \vartheta_{diff}, \qquad \vartheta = \frac{x}{L} \ll \vartheta_{diff} \qquad \left(\vartheta_{diff} \equiv \frac{\hbar}{2\sigma_x} \ll 1\right), \tag{26}$$

i.e. the angle d/L and the observation angle $\vartheta = x/L$ must be smaller than the diffraction angle ϑ_{diff}. Furthermore, the relation $\overline{t} \gg \overline{d} \gg 1$ is equivalent to

$$\frac{L}{R} \gg \frac{d}{\sigma_x} \gg 1 \tag{27}$$

where $R = 2\sigma_x^2/\hbar$ is the Rayleigh range, which is a measure of the divergence of a Gaussian beam, whose transverse width is σ_x. The first of conditions (26) guarantees that particles arrive at the centre of the screen S and, from an optical point of view, equation (27) says that

$$L\frac{\hbar}{\sigma_x} \gg d \tag{28}$$

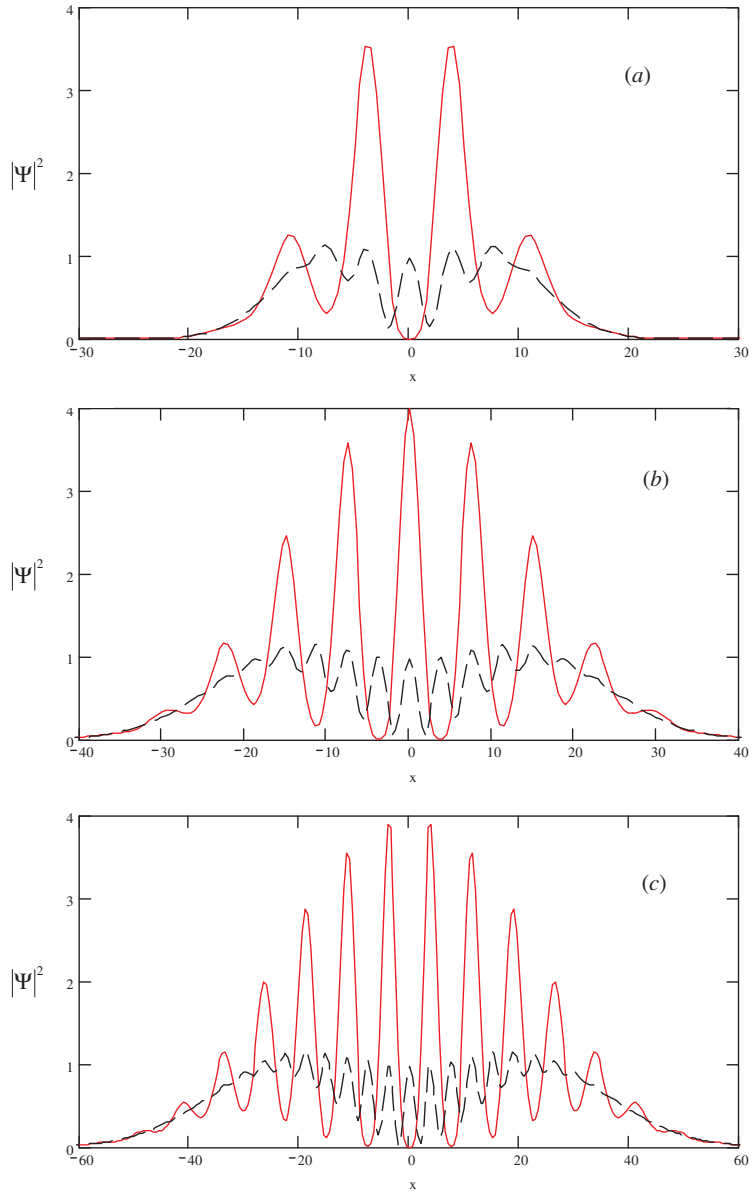

Figure 3. Comparison between three slits (solid curve) and two slits (dashed curve) interference pattern for different values of n, $\overline{t}_n = L_n/R$ and $\overline{d}_n$ (see the text): (*a*) $n = 1, \overline{t}_1 \approx 4.5$ and $\overline{d}_1 \approx 7.7$; (*b*) $n = 2, \overline{t}_2 \approx 9.1$ and $\overline{d}_2 \approx 15.2$; (*c*) $n = 3, \overline{t}_3 \approx 13.6$ and $\overline{d}_3 \approx 22.7$. Notice that, with three slits, for odd n there is zero intensity at the centre, whereas for even n there is a maximum.

i.e. the spread due to diffraction is greater than the spacing between the slits. Finally, notice that equation (10), using the previous definitions, can be written in the form of the well known diffraction envelope:

$$\sqrt{G_+ G_-} \approx \exp\left\{-\frac{x^2(2\sigma_x)^2}{2L^2\lambda^2}\right\} = \exp\left\{-\frac{\vartheta^2}{2\vartheta_{diff}^2}\right\}. \qquad (29)$$

Let us now consider the three-slit case and, in particular, what happens at the centre of the screen. Equation (17) can be rewritten as

$$|\Psi(0,\overline{t})|^2 \propto |1 + 2\sqrt{G}e^{i\Phi}|^2,$$
$$\Phi \equiv \frac{\overline{d}^2}{4(1+\overline{t}^2)}\,\overline{t} \approx \frac{\overline{d}^2}{4\overline{t}}. \qquad (30)$$

Here $\sqrt{G}$ is due to diffraction from silts 1 and 3 (figure 1). The conditions to see zero intensity in $\overline{x} = 0$ are obtained imposing that the sum of the amplitudes coming from slits 1 and 3 (i.e. $2\sqrt{G}$) is equal to the amplitude coming from slit 2 (here normalized to 1) and imposing also that the phase difference is $n\pi$, with odd n (destructive interference). This leads to equations (19) and (20) in the limit $\overline{t} \gg 1$. Now, using the definitions of $\overline{t}$ and $\overline{d}$, the condition $\Phi = n\pi$ (with odd n) can be rewritten as

$$\Delta \equiv \frac{d^2}{2L} = (2n+1)\frac{\lambda}{2} \qquad (31)$$

where Δ is the *path difference* between slits 1 (or 3) and 2. In fact, for $d \ll L$, one has (see figure 1)

$$\Delta \equiv \sqrt{L^2 + d^2} - L \approx \frac{d^2}{2L}, \qquad (32)$$

hence the disappearance of the central peak has a very clear optical interpretation.

4. Decoherence and spontaneous intrinsic decoherence in interference experiments

First, we briefly summarize the model-independent formalism introduced in previous papers [4, 8, 9] to describe decoherence due to fluctuations in the evolution time. The density operator which takes into account these fluctuations is the time average of the usual density operator, i.e.

$$\overline{\rho}(t) = \int_0^\infty \mathrm{d}t'\, \mathcal{P}(t, t', \tau)\rho(t') \tag{33}$$

where the weight function is given by the Γ-distribution function

$$\mathcal{P}(t, t', \tau) = \frac{\exp(-t'/\tau)}{\tau} \frac{(t'/\tau)^{t/\tau - 1}}{\Gamma(t/\tau)}. \tag{34}$$

Here τ is a characteristic time which rules time fluctuations and can also be a function of t [4, 8, 9], and can have experimental or intrinsic origin. In general, if τ is limited by τ_E, one always has a contribution given by intrinsic decoherence.

In the interference case, since $t = L/v$, time fluctuations are induced by velocity spread, as in the case of cavity QED described in [4, 9]. If the system is initially in a pure state, as assumed above, from equation (33) one obtains

$$\overline{P}(\overline{x}, \overline{t}) \equiv \langle \overline{x}|\overline{\rho}(\overline{t})|\overline{x}\rangle = \int_0^\infty \mathrm{d}\overline{t'}\, \mathcal{P}(\overline{t}, \overline{t}', \overline{\tau}) P(\overline{x}, \overline{t}') \tag{35}$$

where the expression of $P(\overline{x}, \overline{t}')$ is given by (6) and (14) in the case of two and three slits, respectively, and $\overline{\tau}$ is given by

$$\overline{\tau} \equiv \frac{\sigma_v}{\sigma_x}\tau, \tag{36}$$

where the scaling (4) has been used for all variables.

We assume τ to be the uncertainty in arrival time of particles at the screen, so that [9, 10]

$$\tau = \frac{\Delta_z(t)}{\overline{\mathcal{V}}} \qquad \text{where } \Delta_z(t) = \sqrt{\sigma_z^2 + \sigma_{\overline{\mathcal{V}}}^2 t^2 + \Delta_{\overline{\mathcal{V}}}^2 t^2},\ t = \frac{L}{\overline{\mathcal{V}}}. \tag{37}$$

Here $\Delta_z(t)$ is the total uncertainty in position along the $\hat{z}$ axis [2], which is obtained summing up the square of two errors: an intrinsic one, $\sigma_z^2 + \sigma_{\overline{\mathcal{V}}}^2 t^2$ (with $\sigma_z \sigma_{\overline{\mathcal{V}}} = \hbar/2m$), i.e. the quantum Schrödinger free-particle spread along the $\hat{z}$ axis, and an 'extrinsic' one, $\Delta_{\overline{\mathcal{V}}}^2 t^2$, i.e. the spread due to classical uncertainty of velocity distribution, e.g. thermal distribution. A more rigorous derivation of equation (37) is given in [9]. Note that τ is always greater than $\tau_E = \sigma_z/\overline{\mathcal{V}} = \hbar/2\sigma(\mathcal{H}_z)$, where $\mathcal{H}_z$ is the kinetic energy along the $\hat{z}$ axis and $\sigma(\mathcal{H}_z)$ its standard deviation, in agreement with equation (1). Assuming t such that $(\sigma_{\overline{\mathcal{V}}}^2 + \Delta_{\overline{\mathcal{V}}}^2)t^2 \gg \sigma_z^2$, from equations (36) and (37) one directly obtains

$$\overline{\tau} = a\overline{t} \qquad \text{with } a = \frac{\sqrt{\sigma_{\overline{\mathcal{V}}}^2 + \Delta_{\overline{\mathcal{V}}}^2}}{\overline{\mathcal{V}}}. \tag{38}$$

If we take $\overline{\tau}/\overline{t} = \tau/t = a \ll 1$, $\mathcal{P}(\overline{t}, \overline{t}', \overline{\tau})$ can be approximated with the Gaussian

$$\mathcal{P}(\overline{t}, \overline{t}', \overline{\tau}) \approx \frac{1}{\sqrt{2\pi\overline{t}\,\overline{\tau}}} \exp\left\{-\frac{(\overline{t} - \overline{t}')^2}{2\overline{t}\,\overline{\tau}}\right\}. \tag{39}$$

In this limit we can perform the average (35) obtaining the analytical expression for the two-slit case:

$$\overline{P}(\overline{x}, \overline{t}) = b(\overline{t})\left\{G_+ + G_- + 2\sqrt{G_+ G_-}\,\mathrm{e}^{-D}\cos\omega\overline{t}\right\} \tag{40}$$

where $b(\overline{t})$ is a normalization factor and

$$D \approx \frac{\overline{x}^2\overline{d}^2}{2}\frac{\overline{\tau}}{\overline{t}^3} = \frac{1}{2}\frac{x^2(2d)^2}{L^2\lambda^2}a \tag{41}$$

where we used equations (4) and (38). The behaviour of $\overline{P}(\overline{x}, \overline{t})$, as a function of $\overline{x}$ at a given $\overline{t} = L/R$, is shown in figure 5 for different values $\overline{d} = d/\sigma_x$ and a. The term e^{-D} is another Gaussian *decoherence envelope not due to diffraction*, as the one of equation (29), *but due to velocity spread*. It is very important to note that it goes as $(2d)^2$, i.e. the square of the distance between slits, as this is typical of decoherence phenomena [5]. In general, the diffraction envelope and the decoherence one are both present in experiments, but the latter becomes visible as soon as $D \geqslant 1$ and it dominates diffraction when

$$a > \left(\frac{\sigma_x}{d}\right)^2 \tag{42}$$

which gives a lower limit to the relative velocity spread a.

We can also write equation (41) as

$$D = \frac{1}{2}\left(\frac{\vartheta}{\vartheta_{int}}\right)^2 a \tag{43}$$

where $\vartheta_{int} = \lambda/2d$ (see equation (25)) and $\vartheta \approx x/L$. If one evaluates D in the interference pattern maxima (25), one obtains

$$D = 2\pi^2 n^2 a. \tag{44}$$

Hence decoherence becomes more and more efficient as n and a increase (see figure 4).

Now, thanks to equation (38) we are able to study the classical and the quantum limit:

(1) in the *classical limit* $\Delta_{\overline{\mathcal{V}}}^2 \gg \sigma_{\overline{\mathcal{V}}}^2$, then equation (43) is ruled by the ratio $a = \Delta_{\overline{\mathcal{V}}}/\overline{\mathcal{V}}$, so that decoherence has a classical origin;

(2) in the *quantum limit*, defined as $\Delta_{\overline{\mathcal{V}}}^2 \ll \sigma_{\overline{\mathcal{V}}}^2$, one has SID due to the quantum velocity spread $\sigma_{\overline{\mathcal{V}}} \geqslant \hbar/2m\sigma_z$.

In this limit $a = \sigma_{\overline{\mathcal{V}}}/\overline{\mathcal{V}}$ and decoherence has an intrinsic, quantum mechanical origin related to HUP.

Moreover, at the macroscopic limit λ becomes very small. However, if one also decreases σ_x, so that λ/σ_x remains constant, the diffraction envelope does not suppress the interference pattern; on the contrary, the decoherence envelope kills interference keeping the distance between slits constant (see equation (41)).

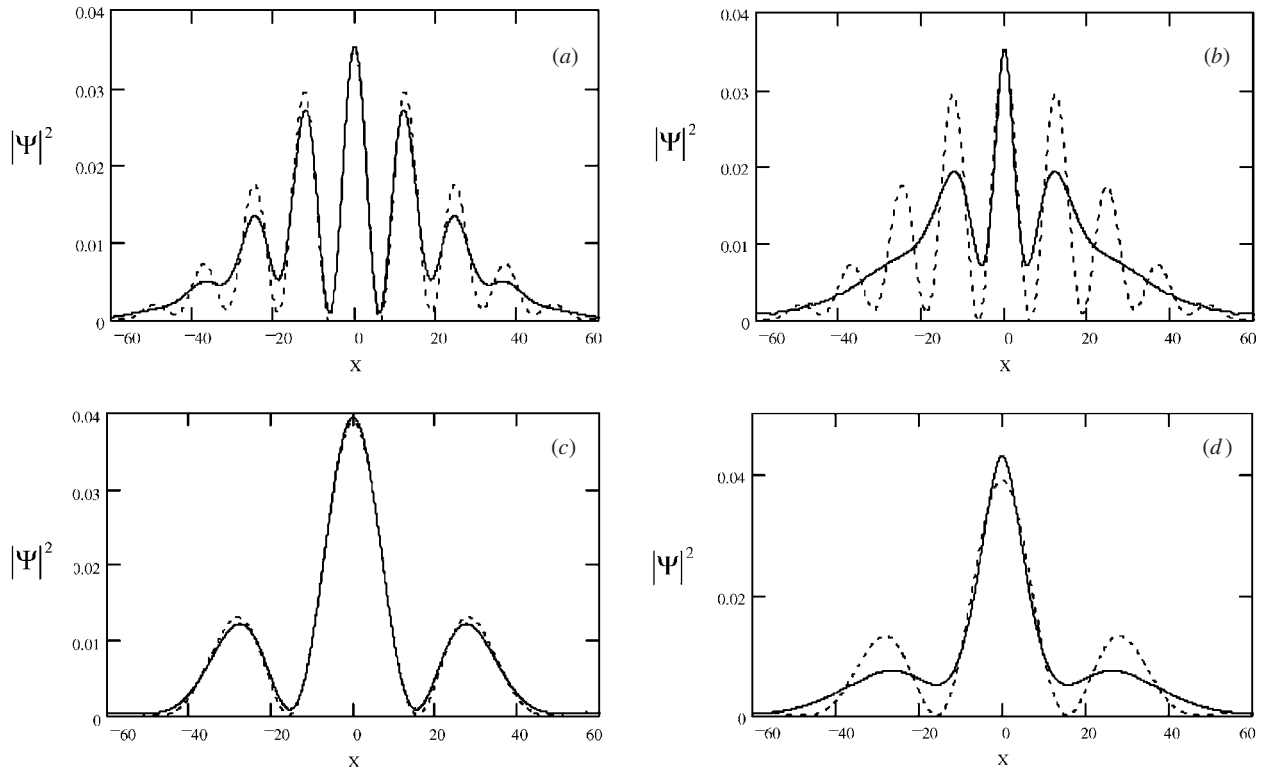

Figure 4. Behaviour of the two-slit interference pattern with decoherence (solid curves) and without decoherence (dotted curves) at time $\overline{t} = L/R = 20$ for different values of d/σ_x and a: (*a*) $d/\sigma_x = 10$, $a = 0.01$; (*b*) $d/\sigma_x = 10$, $a = 0.1$; (*c*) $d/\sigma_x = 4$, $a = 0.01$; (*d*) $d/\sigma_x = 4$, $a = 0.1$.

Finally, when one applies our theory of spontaneous decoherence to the three-slit setup, one proceeds as in the two-slit case, performing the time average of equation (14) and obtaining

$$\overline{P}(\overline{x},\overline{t}) = |\tilde{c}(\overline{t})|^2(G_+ + G_- + G_0 + 2\sqrt{G_+G_-}\mathrm{e}^{-(D_{+,-})}\cos\omega_1\overline{t} + 2\sqrt{G_0G_-}\mathrm{e}^{-(D_{0,-})}\cos\omega_2\overline{t} + 2\sqrt{G_+G_0}\mathrm{e}^{-(D_{0,+})}\cos\omega_3\overline{t}) \tag{45}$$

where $|\tilde{c}(\overline{t})|^2$ is a normalization factor and

$$D_{+,-} \approx \frac{1}{2}\frac{x^2(2d)^2}{L^2\lambda^2}a, \tag{46}$$

$$D_{0,\pm} \approx \frac{1}{2}\frac{(x \pm d/2)^2d^2}{L^2\lambda^2}a, \tag{47}$$

with a given by equation (38). Notice that decoherence still goes as the square of the distance between slits as in the previous case. Therefore, decoherence becomes more efficient with increasing a, and SID becomes observable when the longitudinal quantum velocity spread is dominant, as discussed in the two-slit case. In figure 5 we plotted the comparison of the three-slit interference pattern with and without decoherence for different values of the velocity spread a: fringe visibility is sensibly reduced as soon as $a \sim 10^{-1}$ or greater.

One might think that our results can be easily reproduced just by performing an average with the classical velocity distribution along the $\hat{z}$ axis. However, this would give an expression of the decoherence exponent D similar to equations (43), (46) and (47), but with two basic differences: a^2 instead of a, and a being only a function of the classical contribution $\Delta_{\overline{v}}$. Furthermore, if $a \ll 1$, one will obtain a much smaller decoherence than the one of our approach.

5. Conclusions

We have discussed the single-particle Young interference experiment in position space and we have shown that the interference pattern of a two- and three-slit experiment provides direct evidence of the free-particle Schrödinger spread. Furthermore, in the case of three slits, we demonstrated that for *discrete values of the distances between the slits and of the distance of the screen* it is possible to inhibit particles from reaching the centre of the screen itself, while in the two-slit case there is a maximum of the probability density. Furthermore, we have shown that fringe visibility can be reduced for two different reasons: the usual *diffraction* contribution and a new *decoherence* contribution, which decreases the visibility as the square of the distance between the slits. The decoherence arises from fluctuations in the evolution time $t = L/v$ and, in this paper, such fluctuations are induced by the particle velocity spread as described in cavity QED [4, 9]. The spread *can* have a classical origin (thermal spread and so on) which can be made arbitrarily small with a very monochromatic beam, but it *always* has a finite quantum origin due to the HUP. When this contribution is dominant, one should observe SID, i.e. decoherence not due to interaction with the environment or to experimental fluctuation of some parameter. In general, we find that decoherence is proportional to the *square of the*

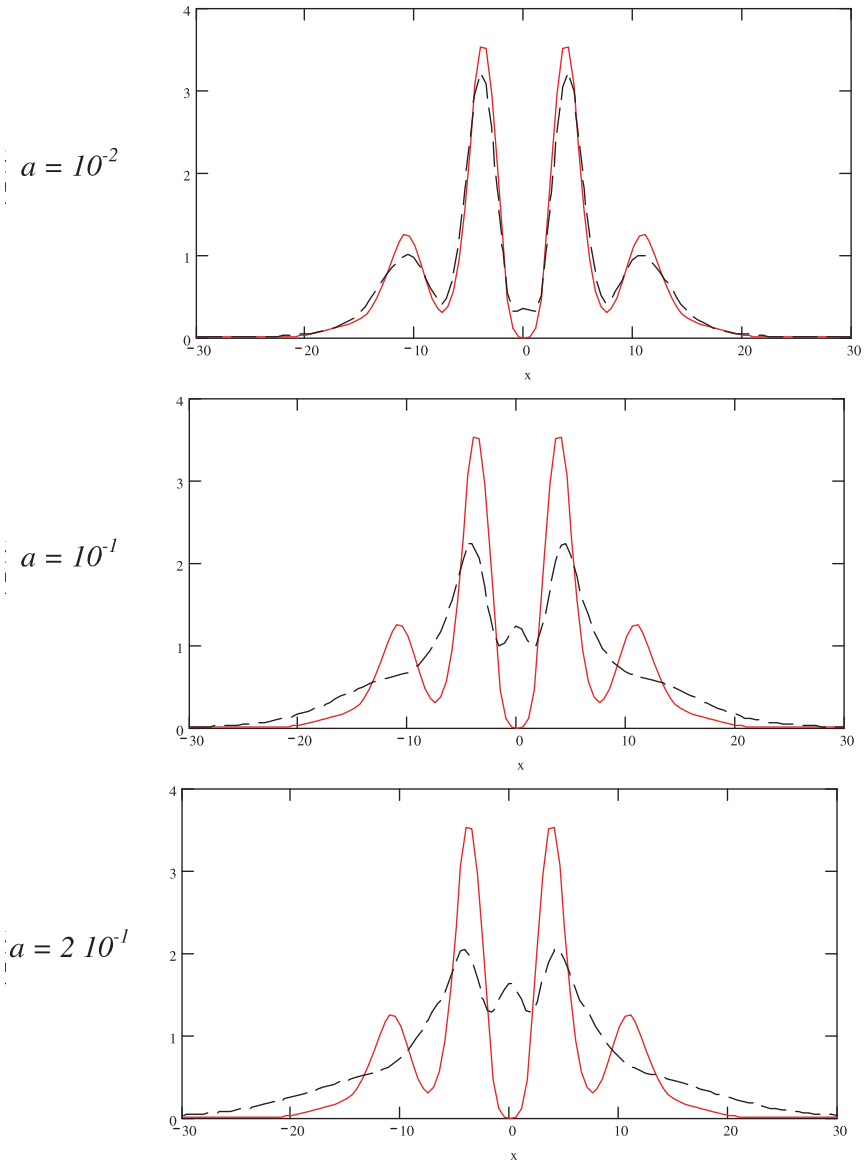

Figure 5. Behaviour of the three-slit interference pattern with decoherence (dashed curve) and without decoherence (solid curve) at time $\overline{t} = L/R \approx 4.5$ and $d/\sigma_x \approx 7.7$ for different values of a (from the top: $a = 10^{-2}$, $10^{-1}$and 2×10^{-1}).

distance of the slits and to the velocity spread parameter a, and becomes very 'efficient' at the macroscopic limit.

References

[1] Feynman R P, Leighton R B and Sands M 1972 *The Feynman Lectures on Physics* vol 3 (Reading, MA: Addison-Wesley)

[2] Bonifacio R and Olivares S 2001 Young's experiment, Schrödinger's spread and spontaneous intrinsic decoherence *Z. Naturf.* a **56** 41–7

[3] Bonifacio R 1999 Time as a statistical variable and intrinsic decoherence *Nuovo Cimento* B **114** 473–88

[4] Bonifacio R, Olivares S, Tombesi P and Vitali D 2000 Model independent approach to nondissipative decoherence *Phys. Rev.* A **61** 053802-1–8

[5] Zurek W H 1991 Decoherence and the transition from quantum to classical *Phys. Today* **44** 36–44 and references therein

[6] Messiah A 1961 *Quantum Mechanics* vol 1 (Amsterdam: North-Holland) ch VIII section 13

[7] Cohen-Tannoudji C *et al* 1977 *Quantum Mechanics* vol 1 (New York: Wiley)

[8] Bonifacio R, Olivares S, Tombesi P and Vitali D 2000 Non-dissipative decoherence in Rabi oscillation experiments *J. Mod. Opt.* **47** 2199–211

[9] Bonifacio R and Olivares S 2001 Spontaneous intrinsic decoherence in Rabi oscillations experiments *Quantum Communication, Computing, and Measurement* vol 3, ed P Tombesi and O Hirota (Dordrecht: Kluwer)

[10] Messiah A 1961 *Quantum Mechanics* vol 1 (Amsterdam: North-Holland) ch IV section 10